# DNA Excited-State Dynamics: Ultrafast Internal Conversion and Vibrational Cooling in a Series of Nucleosides

**Jean-Marc L. Pecourt, Jorge Peon, and Bern Kohler***

*Contribution from the Department of Chemistry, The Ohio State University, 100 West 18th Avenue, Columbus, Ohio 43210*

*Received May 5, 2001*

**Abstract:** To better understand DNA photodamage, several nucleosides were studied by femtosecond transient absorption spectroscopy. A 263-nm, 150-fs ultraviolet pump pulse excited each nucleoside in aqueous solution, and the subsequent dynamics were followed by transient absorption of a femtosecond continuum pulse at wavelengths between 270 and 700 nm. A transient absorption band with maximum amplitude near 600 nm was detected in protonated guanosine at pH 2. This band decayed in 191 ± 4 ps in excellent agreement with the known fluorescence lifetime, indicating that it arises from absorption by the lowest excited singlet state. Excited state absorption for guanosine and the other nucleosides at pH 7 was observed in the same spectral region, but decayed on a subpicosecond time scale by internal conversion to the electronic ground state. The cross section for excited state absorption is very weak for all nucleosides studied, making some amount of two-photon ionization of the solvent unavoidable. The excited state lifetimes of Ado, Guo, Cyd, and Thd were determined to be 290, 460, 720, and 540 fs, respectively (uncertainties are ±40 fs). The decay times are shorter for the purines than for the pyrimidine bases, consistent with their lower propensity for photochemical damage. Following internal conversion, vibrationally highly excited ground state molecules were detected in experiments on Ado and Cyd by hot ground state absorption at ultraviolet wavelengths. The decays are assigned to intermolecular vibrational energy transfer to the solvent. The longest time constant observed for Ado is approximately 2 ps, and we propose that solute−solvent H-bonds are responsible for this fast rate of vibrational cooling. The results show for the first time that excited singlet state dynamics of the DNA bases can be directly studied at room temperature. Like sunscreens that function by light absorption, the bases rapidly convert dangerous electronic energy into heat, and this property is likely to have played a critical role in life's early evolution on earth.

## Introduction

Rising skin cancer rates[1] and anthropogenic modification of the ozone layer[2] have heightened awareness of the health risks of the sun's ultraviolet (UV) rays. It is now well-established that solar UV radiation is the primary cause of nonmelanoma skin cancer.[3] An important factor in photocarcinogenesis is photochemical damage to DNA by direct absorption of UV light.[4] Virtually no UV light with $\lambda < 295$ nm strikes earth's surface due to absorption by stratospheric ozone. As a result, the bases are the only nucleic acid components that can be electronically excited by sunlight. Understanding the excited-state dynamics of the nucleobases is therefore an essential step toward the long-term goal of a molecular-level understanding of DNA photodamage.

As a first step toward understanding photoprocesses in DNA, we have been investigating the photophysics of single nucleosides.[5] The time scale for excited state deactivation by monomeric bases is a crucial input for theories of electronic energy migration in single- and double-stranded DNA. While charge transport in nucleic acids has been widely discussed,[6−16] energy transport[17−20] has received much less attention, despite the latter topic's greater relevance to DNA photobiology. Additionally, the rate of energy transfer between bases is thought to control the distribution of ionic species upon multiphoton ionization of small, hydrated clusters of DNA bases.[21]

* Corresponding author. E-mail: kohler@chemistry.ohio-state.edu. Phone: (614) 688-3944.

(1) Koh, H. K.; Geller, A. C.; Miller, D. R.; Grossbart, T. A.; Lew, R. A. *Arch. Dermatol.* **1996**, *132*, 436.
(2) Young, A. R. *Br. J. Clin. Pract.* **1997**, 10.
(3) Kraemer, K. H. *Proc. Natl. Acad. Sci. U.S.A.* **1997**, *94*, 11.
(4) Mukhtar, H.; Elmets, C. A. *Photochem. Photobiol.* **1996**, *63*, 355.
(5) Pecourt, J.-M. L.; Peon, J.; Kohler, B. *J. Am. Chem. Soc.* **2000**, *122*, 9348; Errata *J. Am. Chem. Soc.* **2001**, *123*, 5166.
(6) Arkin, M. R.; Stemp, E. D. A.; Holmlin, R. E.; Barton, J. K.; Hormann, A.; Olson, E. J. C.; Barbara, P. F. *Science* **1996**, *273*, 475.
(7) Steenken, S. *Biol. Chem.* **1997**, *378*, 1293.
(8) Jortner, J.; Bixon, M.; Langenbacher, T.; Michel-Beyerle, M. E. *Proc. Natl. Acad. Sci. U.S.A.* **1998**, *95*, 12759.
(9) Harriman, A. *Angew. Chem., Int. Ed. Engl.* **1999**, *38*, 945.
(10) Lewis, F. D.; Liu, X.; Liu, J.; Miller, S. E.; Hayes, R. T.; Wasielewski, M. R. *Nature (London)* **2000**, *406*, 51.
(11) Williams, T. T.; Odom, D. T.; Barton, J. K. *J. Am. Chem. Soc.* **2000**, *122*, 9048.
(12) Bixon, M.; Jortner, J. *J. Phys. Chem. B* **2000**, *104*, 3906.
(13) Schuster, G. B. *Acc. Chem. Res.* **2000**, *33*, 253.
(14) Wan, C.; Fiebig, T.; Schiemann, O.; Barton, J. K.; Zewail, A. H. *Proc. Natl. Acad. Sci. U.S.A.* **2000**, *97*, 14052.
(15) Schlag, E. W.; Yang, D. Y.; Sheu, S. Y.; Selzle, H. L.; Lin, S. H.; Rentzepis, P. M. *Proc. Natl. Acad. Sci. U.S.A.* **2000**, *97*, 9849.
(16) Berlin, Y. A.; Burin, A. L.; Ratner, M. A. *J. Phys. Chem. A* **2000**, *104*, 443.
(17) Sutherland, J. C.; Sutherland, B. M. *Biopolymers* **1970**, *9*, 639.
(18) Baverstock, K. F.; Cundall, R. B. *Radiat. Phys. Chem.* **1991**, *37*, 711.
(19) Xu, D. G.; Nordlund, T. M. *Biophys. J.* **2000**, *78*, 1042.
(20) Georghiou, S.; Zhu, S.; Widner, R.; Huang, C. R.; Ge, G. *J. Biomol. Struct. Dyn.* **1990**, *8*, 657.
(21) Kim, N. J.; Kang, H.; Jeong, G.; Kim, Y. S.; Lee, K. T.; Kim, S. K. *J. Phys. Chem. A* **2000**, *104*, 6552.

10.1021/ja0161453 CCC: $20.00 
Published on Web 10/02/2001

The lowest excited singlet ($S_1$) states of the bases lie more than 4 eV above their respective ground states. The substantial energy deposited by light absorption could initiate a variety of photoreactions. For example, electronic excitation transforms any of the bases into a potentially formidable redox partner. The formal excited-state reduction potential of thymine, $E°(\text{Thy}^*/\text{Thy}^{\bullet+}) = 2.1$ V,[22] is high enough to oxidize guanine, $E°(\text{Gua}^{\bullet+}/\text{Gua}) = 1.29$ V at pH 7.[25] Yet, there have been no reports of interbase photoinduced electron transfer by singlet excited states. Additionally, the quantum yields for the formation of pyrimidine (6−4)pyrimidone photoproducts, cyclobutane pyrimidine dimers, and other photoproducts are extremely low.[26−28] Reactive decay channels such as these are made highly improbable by rapid nonradiative decay, which provides DNA with a high level of intrinsic photostability.

The fluorescence quantum yields of the DNA bases were first measured at room temperature in the early 1970s.[24,29] The yields for the DNA nucleosides are $\leq 10^{-4}$. Triplet quantum yields[30] are known less precisely, but are also very small, indicating that nonradiative decay by internal conversion dominates the excited state deactivation. While it has been widely recognized that these emission characteristics imply $S_1$ lifetimes of $\leq 10$ ps,[31] it has not been possible to obtain precise values for any DNA base. This has hampered attempts to understand the mechanism responsible for ultrafast nonradiative decay by the nucleobases.

Most investigators have tried to characterize DNA base excited-state dynamics by measuring emission decays with streak cameras. However, for ultraweak fluorophores like the DNA bases, only a vanishingly small number of photoexcited molecules contribute to an emission signal at any instant. In contrast, a high fraction of the molecules initially excited to the $S_1$ state can be detected by excited-state absorption ($S_1 \rightarrow S_N$ absorption, or ESA) to higher lying singlet states before they decay nonradiatively, if time resolution is sufficient. Nikogosyan pioneered the application of the pump−probe method to nucleic acid photoprocesses.[35−37] Laubereau and co-workers have continued this approach with improved time resolution.[38,39] Unfortunately, the results have been difficult to interpret due to the simultaneous occurrence of single-photon and multiphoton processes. We have recently succeeded in directly detecting ESA in several DNA and RNA nucleosides using femtosecond transient absorption spectroscopy.[5] Here we describe in detail how femtosecond pump−probe measurements made at very low pump intensities have been used to isolate the $S_1$ dynamics from signals arising from multiphoton processes such as water photoionization. By directly observing ultrafast internal conversion and vibrational cooling, the measurements presented here provide a more complete and richly detailed picture of nucleobase photophysics.

## Experimental Methods

**Transient Absorption Spectrometer.** Femtosecond pump−probe experiments were carried out on aqueous solutions of the various nucleosides with use of 150 fs UV pump pulses with a center wavelength of 263 nm. The pump pulse was obtained by third harmonic generation from a kHz-repetition-rate, chirped-pulse amplified titanium: sapphire laser system, as described elsewhere in more detail.[40] The variable wavelength probe pulse was generated by spectrally filtering a continuum with an appropriate interference filter. The continuum generated in a 1 cm water cell by the laser fundamental provided probe light at wavelengths between 400 and 700 nm, while the laser system's second harmonic was used to generate a UV continuum in a 1 mm $CaF_2$ glass flat for probing at $\lambda < 400$ nm. Pump and probe pulses were focused and crossed in a free-flowing, liquid jet of the solution under study. All measurements were carried out at room temperature ($T = 22 \pm 1$ °C).

The pump pulse was linearly polarized by using a Glan-Taylor polarizer made from $\beta$-barium borate because this material has higher UV transmission than calcite. A half-wave plate positioned immediately before the polarizer was used to vary the pump pulse energy for intensity-dependent studies. The $1/e^2$ beam radius of the focused pump pulse at the sample was measured to be 170 $\mu$m by the scanning knife-edge method.[41] The probe pulse spot size was 3−4 times smaller. The polarizations of the pump and probe pulses were set to the magic angle to eliminate reorientational dynamics.

Transient absorption signals were recorded with use of a lock-in amplifier referenced to a chopper that synchronously blocked every third pump pulse. The transmitted probe pulse was detected with an amplified silicon photodiode or a photomultiplier tube, depending on wavelength. The induced absorbance change ($\Delta A$, equivalent to $\Delta$OD) was recorded versus time delay between pump and probe pulses. $\Delta A$ is defined as the sample absorbance at the probe wavelength in the presence of the pump pulse minus the absorbance at the same wavelength with the pump blocked. Our instrument can routinely measure absorbance changes as small as 10−20 ppm, and this high sensitivity was essential for detecting the weak ESA from the nucleosides.

**Chemicals.** The RNA nucleosides adenosine (Ado), cytidine (Cyd), and guanosine (Guo) and the DNA nucleoside thymidine (Thd) were obtained from Sigma Chemical Co. and used as received. Nucleosides were selected for this study rather than the free bases because of their greater solubility in water. Additionally, the (deoxy)ribose group of the nucleosides eliminates some tautomers, reducing ground-state heterogeneity. Some measurements were also performed with the mononucleotide guanosine 5′-monophosphate (GMP), which was also purchased from Sigma. Solutions were prepared with ultrapurified water from a commercial water purification system (Barnstead Nanopure). Identical results were obtained with HPLC-grade water (Aldrich). The nucleosides were usually studied in unbuffered solutions at approximately pH neutral conditions. The lack of a pH buffer is most likely to affect results for Cyd, on account of its high p$K_a$ of 4.2[42] for

(22) This value (vs NHE) is calculated from the literature value for the reduction potential of thymine, $E°(\text{Thy}/\text{Thy}^{\bullet-}) = -2.18$ V,[23] and its singlet energy of 4.28 eV.[24]

(23) Seidel, C. A. M.; Schulz, A.; Sauer, M. H. M. *J. Phys. Chem.* **1996**, *100*, 5541.
(24) Daniels, M.; Hauswirth, W. *Science* **1971**, *171*, 675.
(25) Steenken, S.; Jovanovic, S. V. *J. Am. Chem. Soc.* **1997**, *119*, 617.
(26) Cadet, J.; Vigny, P. In *Bioorganic Photochemistry*; Morrison, H., Ed.; Wiley: New York, 1990; Vol. 1, p 1.
(27) Lemaire, D. G. E.; Ruzsicska, B. P. *Photochem. Photobiol.* **1993**, *57*, 755.
(28) Görner, H. *J. Photochem. Photobiol. B: Biol.* **1994**, *26*, 117.
(29) Vigny, P. *C. R. Acad. Sci., Ser. D* **1971**, *272*, 3206.
(30) Daniels, M. In *Photochemistry and Photobiology of Nucleic Acids*; Wang, S. Y., Ed.; Academic Press: New York, 1976; Vol. 1, p 23.
(31) For reviews of DNA photophysics see refs 26, 30, and 32−34.
(32) Vigny, P.; Duquesne, M. In *Excited States of Biological Molecules*; Birks, J. B., Ed.; Wiley: New York, 1976; Vol. 3, p 167.
(33) Callis, P. R. *Annu. Rev. Phys. Chem.* **1983**, *34*, 329.
(34) Ruzsicska, B. P.; Lemaire, D. G. E. In *CRC handbook of organic photochemistry and photobiology*; Horspool, W. M., Song, P.-S., Eds.; CRC Press: Boca Raton, FL, 1995; p 1289.
(35) Oraevsky, A. A.; Sharkov, A. V.; Nikogosyan, D. N. *Chem. Phys. Lett.* **1981**, *83*, 276.
(36) Nikogosyan, D. N.; Oraevsky, A. A.; Letokhov, V. S.; Arbieva, Z. K.; Dobrov, E. N. *Chem. Phys.* **1985**, *97*, 31.
(37) Nikogosyan, D. N.; Angelov, D.; Soep, B.; Lindqvist, L. *Chem. Phys. Lett.* **1996**, *252*, 322.
(38) Reuther, A.; Nikogosyan, D. N.; Laubereau, A. *J. Phys. Chem.* **1996**, *100*, 5570.
(39) Reuther, A.; Iglev, H.; Laenen, R.; Laubereau, A. *Chem. Phys. Lett.* **2000**, *325*, 360.
(40) Peon, J.; Hess, G. C.; Pecourt, J.-M. L.; Yuzawa, T.; Kohler, B. *J. Phys. Chem. A* **1999**, *103*, 2460.
(41) Arnaud, J. A.; Hubbard, W. M.; Mandeville, G. D.; de la Clavière, B.; Franke, E. A.; Franke, J. M. *Appl. Opt.* **1971**, *10*, 2775.
(42) Bloomfield, V. A.; Crothers, D. M.; Tinoco, I., Jr. *Physical Chemistry of Nucleic Acids*; Harper & Row: New York, 1974.

protonation. We found, however, that signals for Cyd are independent of pH when the pH was varied between 4 and 8 by addition of HCl or NaOH. The signals reported here for unbuffered conditions are therefore assumed to accurately characterize the dynamics of the neutral nucleosides.

Solute concentrations were in the 3−4 mM range, except for Guo, the least soluble of the nucleosides. Solutions of Guo were prepared at neutral pH by gently heating an aqueous solution to 70 °C under stirring. In this way, a supersaturated solution with a concentration of approximately 1 mM could be prepared and studied for up to an hour before significant solute precipitation occurred. The absorbance at the pump wavelength was roughly unity for Ado, Cyd, and Thd. In the case of Guo, the absorbance was 0.5. All solutions were recirculated through a home-built nozzle that formed a liquid jet with a path length of approximately 0.4 mm. The flow rate was high enough to expose a fresh portion of the solution to each successive pair of pump and probe pulses. Solutions were not deaerated because bimolecular quenching by oxygen ($[O_2] \approx 0.3$ mM at 20 °C in $H_2O$) occurs on a time scale of hundreds of nanoseconds even for diffusion-limited quenching.

**Global Curve Fitting.** Transient signals were fit to a sum of exponentials by using our own implementation of a global, nonlinear least-squares fitting program. The fitting function was analytically convoluted with a Gaussian (fwhm 210 fs) that best represents the instrument response function. Small changes to the width of this Gaussian had no significant effect on the time constants reported below. In global fitting, temporal decay curves at different probe wavelengths are fit simultaneously under the constraint that one or more parameters of the fitting function must take on common ("global") values for all curves.[43] In our case, the exponential time constants were globally constrained, while the amplitudes were allowed to vary independently. Global fitting greatly improves the precision of exponential decay times estimated from time- and wavelength-resolved data.[43]

## Results

**Transient Absorption at Visible Probe Wavelengths.** The singlet excited states of any molecule are more closely spaced as energy is increased.[44] As a result, $S_1 \rightarrow S_N$ transitions usually lie at longer wavelengths than absorption bands of the electronic ground state, $S_0$. For this reason, we began our search for base ESA at visible wavelengths. Our first measurements were performed on aqueous solutions of Guo at low pH. Protonated Guo ($GuoH^+$) is significantly more fluorescent than Guo. The well-characterized fluorescence lifetime[45] provided a reliable criterion for identifying ESA by the fluorescent state (see Discussion section).

Transient absorption by Guo at pH 2 is shown at 570 nm in Figure 1. After an instrument-limited rise, the signal decays biexponentially. Transients with identical kinetics were detected at probe wavelengths between 450 and 700 nm, with the largest signals near 600 nm. Transients at five separate probe wavelengths were globally fit to a sum of two exponentials. The best-fit values of the exponential time constants, $\tau_1 = 1.7 \pm 0.3$ ps and $\tau_2 = 191 \pm 4$ ps, gave an excellent fit at all probe wavelengths. The longer time constant agrees extremely well with the emission lifetime of $196 \pm 7$ ps reported by Fujiwara et al.[45] These authors studied Guo at pH 2 using excitation pulses at 263 nm and a synchroscan streak camera. This agreement indicates that the slower decay component of the transient absorption signal is due to absorption by the fluorescent (i.e. $S_1$) state of $GuoH^+$.

The remaining measurements were performed at approximately neutral pH. ESA by $GuoH^+$ turned out to be a good predictor of $S_1 \rightarrow S_N$ absorption by the neutral nucleosides, and a broad transient absorption band with a maximum near 600 nm was located for each compound. Signals recorded for Guo at pH $\approx$ 7 are shown in Figure 2 at three probe wavelengths. The dominant feature of the transients in Figure 2 is the subpicosecond decay. At delay times greater than 2 ps, a small offset is visible in each trace. The decays at all probe wavelengths were simultaneously fit to a single exponential plus a constant to model the residual absorption at long times. The exponential time constant ($\tau$) was adjusted globally, while the amplitude and constant were adjusted independently for each transient. The best-fit value for $\tau$ is $460 \pm 40$ fs.

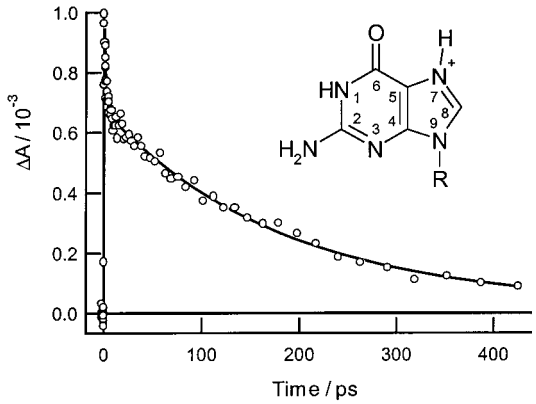


**Figure 1.** Transient absorption (263 nm pump, 570 nm probe) of a 3 mM solution of guanosine in water at pH 2. The inset shows the structure and ring numbering of protonated guanosine. R stands for ribose.

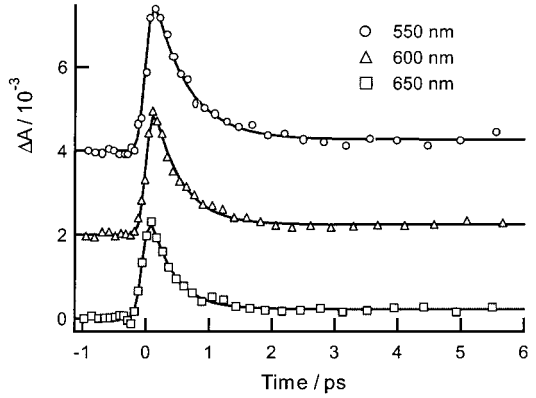


**Figure 2.** Transient absorption from a 1.4 mM solution of guanosine at pH 7 induced by a 263 nm pump pulse. The probe wavelengths are 550 (circles), 600 (triangles), and 650 nm (squares). The curves have been offset vertically for clarity. Global, nonlinear least-squares fits are shown by the solid curves.

To investigate the offset, which was observed for all nucleosides, pump−probe signals were recorded as a function of pump energy. Four representative transients are shown for Ado in Figure 3. These transients were recorded at pump intensities between 2 and 46 GW $cm^{-2}$, and have been scaled to have the same maximum amplitude. Strong reshaping as a function of pump intensity is clearly evident. Similar results were observed for all nucleosides studied. Analysis shows that the signal near zero delay time ($t = 0$) varies linearly with pump pulse intensity, while the long-time offset varies quadratically. Thus, the subpicosecond decay is due to one-photon excitation, while the constant signal seen afterward results from two-photon excitation.

Transient spectra were assembled point-wise from signals recorded at single wavelengths. Results are shown for Cyd in

(43) Knutson, J. R.; Beechem, J. M.; Brand, L. *Chem. Phys. Lett.* **1983**, *102*, 501.

(44) Klessinger, M.; Michl, J. *Excited States and Photochemistry of Organic Molecules*; VCH: New York, 1995.

(45) Fujiwara, T.; Kamoshida, Y.; Morita, R.; Yamashita, M. *J. Photochem. Photobiol. B: Biol* **1997**, *41*, 114.

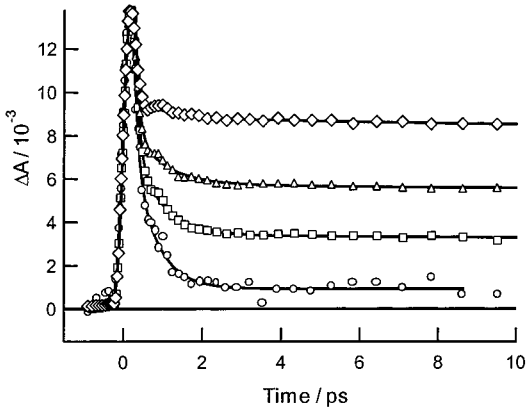


**Figure 3.** Intensity dependence of the transient absorption signal at 570 nm from a 4.0 mM adenosine solution at pH ≈7. The pump intensities are 46 (diamonds), 16 (triangles), 8.0 (squares), and 2.0 GW $cm^{-2}$ (circles). The signals at the three lowest intensities have been scaled to agree with the peak of the 46 GW $cm^{-2}$ trace at short times. Global, nonlinear least-squares fits are shown by the solid curves.

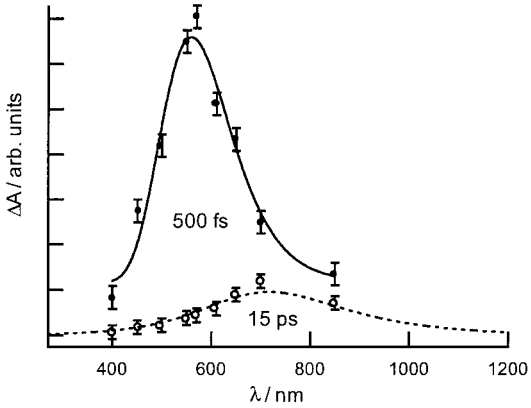


**Figure 4.** Transient spectra from a 4.3 mM aqueous solution of cytidine recorded 500 fs and 15 ps after excitation with a 150 fs, 263 nm pump pulse. The solid curve was obtained by fitting a Gaussian to the short-time spectrum plotted vs frequency. The dashed curve is the absorption spectrum of the solvated electron [from: Jou, F.-Y.; Freeman, G. R. *J. Phys. Chem.* **1979**, *83*, 2383].

Figure 4. The transient spectrum 500 fs after the pump pulse (closed circles) has $\lambda_{max} \approx 560$ nm and is considerably narrower than the red-shifted spectrum measured at 15 ps delay (open circles). As a guide to the eye, the solid line through the open circles displays a Gaussian fit to the short time spectrum plotted vs frequency. Similar short-time spectra with a broad peak between 500 and 600 nm were observed for the other nucleosides. The different spectra and the different intensity dependence at early and late times indicate that the species contributing to the probe absorption are not the same at all delay times. The dashed curve in Figure 4 shows the well-known spectrum of the hydrated electron, $e_{aq}^-$, scaled to agree with the maximum amplitude of the 15 ps spectrum. The agreement is excellent, indicating that absorption at long times originates from $e_{aq}^-$.

The pump-power dependence indicates that hydrated electrons are produced by two-photon absorption. To determine the source of the electrons, transients were recorded at 600 nm for a range of solute concentrations, while maintaining constant pump intensity. The nucleotide guanosine-5′-monophosphate (GMP) was used for this study because it is much more soluble than Guo. Figure 5 displays the transients obtained when the GMP concentration was varied by a factor of ≈16. The ratio of the offset to the signal maximum is largest at low GMP concentrations. The inset to this figure shows how the absolute signal

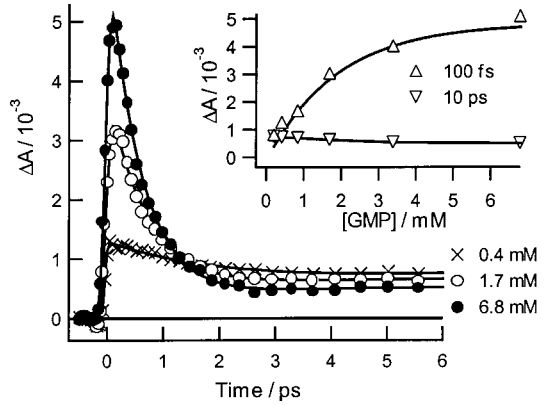


**Figure 5.** Transient absorption at 600 nm for guanosine 5′-monophosphate (GMP) as a function of solute concentration. The pump intensity was 5 GW $cm^{-2}$ for each scan. The inset shows the variation of the absolute signal strength with GMP concentration at two different delay times.

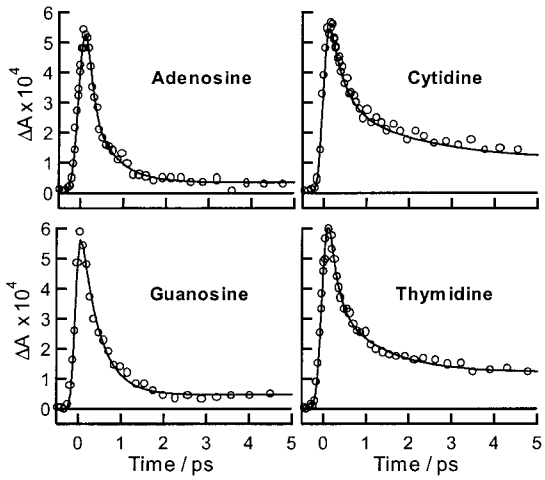


**Figure 6.** Transient absorption (263 nm pump, 570 nm probe) for all nucleosides studied. The pump intensity was kept as low as possible to minimize interference by the hydrated electron. The pump intensity was 8.3 GW $cm^{-2}$ for the pyrimidine bases and 3.5 GW $cm^{-2}$ for the purine bases.

changes 100 fs and 10 ps after the pump pulse. The short-time signal increases dramatically, while the long-time signal actually decreases as the solute concentration is increased.

To isolate the monophotonic dynamics from the multiphoton signal component, pump−probe scans were carried out on all nucleosides at neutral pH at the lowest possible pump intensities that still resulted in acceptable signal-to-noise ratios. The results are shown in Figure 6. The pump pulse energy was fixed at 250 nJ for the purine nucleosides (Ado and Guo), corresponding to a pump intensity of 3.5 GW $cm^{-2}$. The traces for the pyrimidine nucleosides (Cyd and Thd), which absorb more weakly at short times, were obtained with a pump pulse energy of 600 nJ (8.3 GW $cm^{-2}$). Global fitting to low-power signals at several probe wavelengths was performed by using a model function consisting of a single exponential and a constant. The best-fit decay times are summarized in Table 1.

**Transient Absorption at UV Probe Wavelengths.** In contrast to the signals observed in the visible, signals at UV probe wavelengths are significantly more intense, and exhibit slower dynamics. Results are shown in Figures 7 and 8 for Ado and Cyd. Figure 7a shows the transients for Ado on an absolute absorbance scale. In Figure 7b the same transients have been normalized to have the same maximum amplitude. The transients

**Table 1.** $S_1$ Lifetimes and Initial Vibrational Temperatures in $H_2O$ at $T = 22$ °C

| nucleoside | $\tau^a$/fs | $T_{vib}{}^b$/K | $T_{vib}{}^c$/K |
|---|---|---|---|
| adenosine | 290 | 1232 | 1177 |
| guanosine | 460 | 1203 | 1121 |
| cytidine | 720 | 1292 | 1208 |
| thymidine | 540 | 1272 | 1190 |

[a] $S_1$ lifetime (±40 fs, 95% confidence). [b] Vibrational temperature calculated from eq 2. [c] Vibrational temperature calculated from eq 3, using electronic (0−0) transition energies from ref 26.

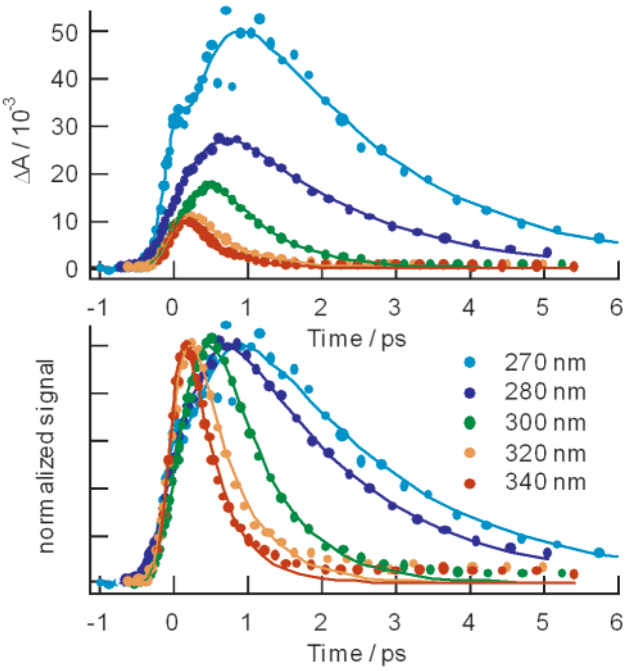


**Figure 7.** Transient absorption for adenosine at UV probe wavelengths on an absolute (a) and normalized intensity scale (b).

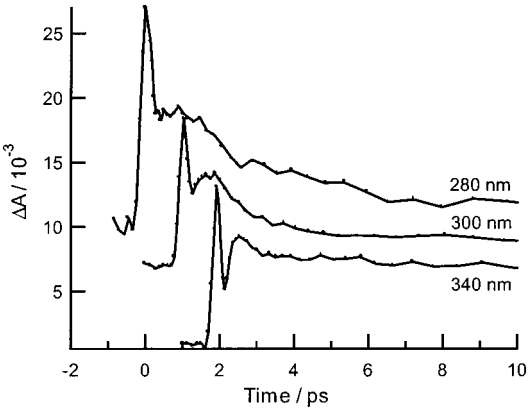


**Figure 8.** Transient absorption for cytidine in the UV. Traces have been offset horizontally and vertically for clarity.

between 270 and 340 nm clearly cannot be globally fit to a single time constant. Decay time and signal strength increase dramatically as the probe wavelength is decreased. Individual fits to the transients for Ado are shown in Figure 7 by the solid lines. The fitting function consisted of two exponentials and a delta function (to model the spike at $t = 0$) convoluted with the instrument response. The time constant of the exponential describing the decaying portion of each curve steadily increases from 0.4 ps at 340 nm to 2.0 ps at 270 nm.

Signals at several UV probe wavelengths are shown in Figure 8 for Cyd. As for Ado, stronger, more slowly decaying signals are observed for Cyd in the UV compared to the visible. The signals in Figure 8 were recorded with higher intensity pump and probe pulses than was the case for Ado in Figure 7. Under these conditions an instrument-limited spike at $t = 0$ is prominent. A weaker spike can be seen in the UV transients for Ado, particularly at 270 nm, where a shoulder is evident near $t = 0$. The higher pump intensity used for the Cyd signals in the UV also results in a pronounced offset at long times, which increases at longer wavelengths.

## Discussion

**Internal Conversion from $S_1$ to $S_0$.** At low pH Guo is substantially more fluorescent than at pH 7.[46] This increased fluorescence is due to protonation at N7 (see Figure 1 for ring numbering),[46,47] and is consistent with the greater fluorescent character of other 7-substituted purine nucleosides.[48,49] Consistent with the enhanced emission, the $S_1$ lifetimes for 7-substituted purines are relatively long, and easily measured by streak camera methods. Georghiou et al. measured a fluorescence lifetime of 180−210 ps for 7-methyl GMP.[50] More recently, Fujiwara et al. measured a lifetime of 196 ± 7 ps for $GuoH^+$.[45] This value is in excellent agreement with our best-fit decay time of $\tau = 191 \pm 4$ ps, confirming that the slowly decaying signal component in Figure 1 is due to absorption by the $S_1$ state (fluorescent state) of $GuoH^+$.

The biexponential character of the signal in Figure 1 is due to the presence of Guo and $GuoH^+$. From the reported p$K_a$ of 2.2,[46] a solution at pH 2 is predicted to contain 61% $GuoH^+$ and 39% Guo. The slow decay component reflects excited-state decay by $GuoH^+$ and the 1.7 ps decay component is assigned to excited-state decay by Guo, which is seen in Figure 2 to undergo much more rapid decay at pH 7. From the least-squares fits the amplitude of the slow component varied between 65 and 85% as the probe wavelength was varied across the $S_1 \rightarrow S_N$ absorption band. This is in reasonable agreement with the concentration of $GuoH^+$ estimated from the p$K_a$, and suggests that ESA by the $S_1$ states of the protonated and unprotonated forms is similar in shape and amplitude. The 1.7 ps decay component in Figure 1 is substantially longer than the 0.46 ps lifetime measured for neutral Guo at pH ≈ 7 (Figure 2). Since the $S_1$ lifetime of Cyd did not change when the pH was varied between 4 and 8, excited state deactivation of Guo is unlikely to be affected by pH, especially in view of the short excited-state lifetime. Instead, the disagreement may be due to the uncertainty in fitting the shorter time constant of a biexponential decay.

The removal of a single proton from $GuoH^+$ shortens the lifetime of the transient absorption signal by a factor of over 400, as shown in Figure 2. The other nucleosides also show subpicosecond decays at pH 7, as seen in Figure 6. On the basis of the intensity-dependent results, the short-time dynamics clearly originate from one-photon excitation of the nucleosides. We considered and rejected other assignments of the short-time dynamics. The triplet states of the bases have microsecond lifetimes,[26] ruling out triplet−triplet absorption. The signals also cannot be due to aggregates since the association constants determined by vapor-phase osmometry predict negligible aggregation in aqueous solution for the millimolar nucleoside concentrations used here.[51] If the signal arose from base dimers,

(46) Börresen, H. C. *Acta Chem. Scand.* **1963**, *17*, 921.
(47) Tsuboi, M.; Kyugoku, Y.; Shimanouchi, T. *Biochim. Biophys. Acta* **1962**, *55*, 1.
(48) Jones, J. W.; Robins, R. K. *J. Am. Chem. Soc.* **1963**, *85*, 193.
(49) Wilson, R. W.; Callis, P. R. *Photochem. Photobiol.* **1980**, *31*, 323.
(50) Georghiou, S.; Nordlund, T. M.; Saim, A. M. *Photochem. Photobiol.* **1985**, *41*, 209.

then it should increase as the square of the solute concentration. We found, however, that the short-time signal was always strictly proportional to the absorbance by the nucleoside at the pump wavelength when the solute concentration was varied, as shown in the inset to Figure 5. The short-time signals are assigned then to dynamics of the $S_1$ states of the nucleosides, which are populated by the absorption of a single pump photon. The spectral similarity between the $S_1 \rightarrow S_N$ absorption bands of Guo and $GuoH^+$ further indicates that the fast signals at pH 7 are due to ESA. The subpicosecond decays observed for all nucleosides (Figure 6) therefore reflect internal conversion from $S_1$ to $S_0$.

From the transient spectrum recorded 15 ps after the pump pulse (Figure 4), absorption by $e_{aq}^-$ is responsible for the offset. For our pump wavelength of 263 nm, two-photon absorption prepares an excited state with an energy of 9.4 eV. This energy is higher than the vertical ionization potentials reported by Hush and Cheung for the DNA bases in the gas phase.[52] Solvation results in a substantial lowering of the ionization thresholds of neutral molecules in aqueous solution, and the nucleosides Ado, Guo, and dCyd have all been reported to undergo monophotonic ionization in water at 193 nm (6.4 eV).[53] Although the ionization potential of water in the gas phase lies well above 9.4 eV, it is well-established that $e_{aq}^-$ is produced in bulk water at excitation energies as low as 6−6.5 eV.[54−56] Ionization of both solute and solvent is thus energetically allowed.

The assignment of $e_{aq}^-$ production to solvent photoionization is definitively established by the concentration-dependent results in Figure 5. As the GMP concentration is increased at constant pump intensity, the offset decreases, indicating that fewer $e_{aq}^-$ are produced. This is the opposite of the expected behavior if two-photon ionization of the solute were dominant. The results in Figure 5 can be modeled by considering only one-photon absorption by the solutes, and two-photon absorption by the much larger number of solvent molecules. Since two-photon absorption depends quadratically, whereas one-photon absorption depends linearly on light intensity, one- and two-photon absorption depend differently on distance along the propagation direction through the liquid jet. The exponential attenuation of photon flux with distance by the one-photon absorbers decreases the total number of two-photon excited states that are produced throughout the sample thickness.

Two-photon ionization of water is promoted by two factors. First, water has a large cross section for two-photon absorption in the UV.[54] Second, the quantum efficiency for electron ejection from states reached by two-photon excitation is high. Bartels and Crowell reported that water-excited states with a final energy of 9.3 eV are photoionized with 50% probability.[57] Working at lower pump intensity reduces the amount of solvent photoionization faster than it reduces the number of monophotonically excited solute molecules. Nevertheless, the minimum detectivity of our instrument ($\Delta A \approx 2 \times 10^{-5}$) prevents us from lowering the pump intensity below a few GW $cm^{-2}$. This is a direct consequence of the strong absorption cross section of $e_{aq}^-$ ($\epsilon_{630\ nm} = 14\,400\ M^{-1}\ cm^{-1}$ [58]) and the small cross section for ESA by the nucleosides. Modeling suggests an upper limit of about 1000 $M^{-1}\ cm^{-1}$ for the molar absorption coefficients of the purine nucleosides. Absorption coefficients for the pyrimidine bases are estimated to be a factor of 3 smaller, and this is the reason for the larger offset for Cyd and Thd in Figure 6.

**Hot Ground-State Absorption and Vibrational Cooling Dynamics in $S_0$.** The assignment of the dynamics at visible probe wavelengths to ultrafast internal conversion is strongly supported by transient absorption measurements in the UV. Figures 7 and 8 show the substantially more intense signals observed at wavelengths on the red edge of the ground-state absorption bands of Ado and Cyd. The kinetics are much slower in the UV than in the visible, suggesting that different states are responsible. This is confirmed by measurements of the time zero anisotropies for Ado. The visible band has a time-zero anisotropy of 0.15, while a value of ≈0.4 was measured for the UV band at 280 nm. The difference indicates that distinct electronic transitions are responsible for the signals in the visible and in the UV.

We assign the UV band to absorption by hot ground-state molecules that are formed by internal conversion. This explains the initial anisotropy of 0.4 since probe absorption in the UV monitors the same electronic transition excited by the pump pulse. In a nonradiative electronic transition, the energy in an excited molecule is not removed by an emitted photon, but instead remains localized in the molecule and its immediate environment. Due to the high-lying $S_1$ states of the bases (average $S_1$ energy is ≈34 000 $cm^{-1}$ in room-temperature aqueous solution[24]), molecules that internally convert from $S_1$ to $S_0$ are vibrationally very highly excited. The large vibrational excess energy results in a pronounced red-shift of the ground-state absorption spectrum. This explains the strong absorption signals seen at wavelengths on the red edge of the $S_0 \rightarrow S_1$ absorption band. This "red edge" or "hot band" absorption has been observed previously in molecules for which electronic relaxation is more rapid than vibrational energy dissipation to the solvent. Examples include azulene[59−63] and linear polyenes such as hexatriene.[64,65] As vibrational energy is transferred to nearby solvent molecules, the solute's vibrational temperature decreases and the electronic absorption spectrum returns to its room-temperature band shape. The rate of this vibrational cooling process is obtained from the decays at UV probe wavelengths. The decay times obtained by fitting the transients in Figures 7 and 8 vary strongly with probe wavelength. This is a common signature of vibrational cooling in ultrafast transient absorption spectroscopy,[66,67] and further justifies our interpretation.

It is usually assumed that intramolecular vibrational redistribution (IVR) occurs rapidly enough after initial photoexci-

(51) Ts'o, P. O. P.; Melvin, I. S.; Olson, A. C. *J. Am. Chem. Soc.* **1963**, *85*, 1289.
(52) Hush, N. S.; Cheung, A. S. *Chem. Phys. Lett.* **1975**, *34*, 11.
(53) Candeias, L. P.; Steenken, S. *J. Am. Chem. Soc.* **1992**, *114*, 699.
(54) Nikogosyan, D. N.; Oraevsky, A. A.; Rupasov, V. I. *Chem. Phys.* **1983**, *77*, 131.
(55) Bernas, A.; Ferradini, C.; Jay-Gerin, J.-P. *Chem. Phys.* **1997**, *222*, 151.
(56) Bernas, A.; Ferradini, C.; Jay-Gerin, J.-P. *J. Photochem. Photobiol. A: Chem.* **1998**, *117*, 171.
(57) Bartels, D. M.; Crowell, R. A. *J. Phys. Chem. A* **2000**, *104*, 3349.
(58) Michael, B. D.; Hart, E. J.; Schmidt, K. H. *J. Phys. Chem.* **1971**, *75*, 2798.
(59) Schwarzer, D.; Troe, J.; Schroeder, J. *Ber. Bunsen-Ges. Phys. Chem.* **1991**, *95*, 933.
(60) Schwarzer, D.; Troe, J.; Votsmeier, M.; Zerezke, M. *J. Chem. Phys.* **1996**, *105*, 3121.
(61) Schwarzer, D.; Troe, J.; Votsmeier, M.; Zerezke, M. *Ber. Bunsen-Ges. Phys. Chem.* **1997**, *101*, 595.
(62) Diau, E. W.-G.; DeFeyter, S.; Zewail, A. H. *J. Chem. Phys.* **1999**, *110*, 9785.
(63) Wurzer, A. J.; Wilhelm, T.; Piel, J.; Riedle, E. *Chem. Phys. Lett.* **1999**, *299*, 296.
(64) Pullen, S. H.; Anderson, N. A.; Walker, L. A., II; Sension, R. J. *J. Chem. Phys.* **1997**, *107*, 4985.
(65) Anderson, N. A.; Pullen, S. H.; Walker, L. A., II; Shiang, J. J.; Sension, R. J. *J. Phys. Chem. A* **1998**, *102*, 10588.
(66) Miyasaka, H.; Hagihara, M.; Okada, T.; Mataga, N. *Chem. Phys. Lett.* **1992**, *188*, 259.
(67) Hess, G. C.; Kohler, B.; Likhotvorik, I.; Peon, J.; Platz, M. S. *J. Am. Chem. Soc.* **2000**, *122*, 8087.

tation that a Boltzmann population distribution is established before there is significant intermolecular vibrational energy transfer to the solvent.[68,69] Under these conditions a vibrational temperature can be meaningfully assigned to quantify a molecule's excess vibrational energy. In the harmonic approximation, the mean vibrational energy of an *N*-atom polyatomic molecule in excess of its zero-point energy depends on temperature as,

$$E_{\mathrm{vib}}(T) = \sum_{i=1}^{3N-6} h\upsilon_i \left[ \exp\left(\frac{h\upsilon_i}{k_B T}\right) - 1 \right]^{-1} \quad (1)$$

where $\upsilon_i$ are the $3N - 6$ normal-mode frequencies. If the total photon energy, $E_{\mathrm{photon}}$, remains in the molecule prior to internal conversion, then the initial vibrational temperature, $T$, is the solution to eq 2. If vibrational excess energy in $S_1$ is lost to the

$$E_{\mathrm{vib}}(T) = E_{\mathrm{vib}}(295\ \mathrm{K}) + E_{\mathrm{photon}} \quad (2)$$

solvent before internal conversion, then $E_{\mathrm{photon}}$ must be replaced by the 0−0 transition energy, $E_{0-0}$,

$$E_{\mathrm{vib}}(T) = E_{\mathrm{vib}}(295\ \mathrm{K}) + E_{0-0} \quad (3)$$

Little information is available on the rate of intermolecular vibrational energy transfer in the condensed phase, particularly in excited states, so we computed initial vibrational temperatures using both eqs 2 and 3. Normal-mode frequencies were calculated for the electronic ground state of each nucleoside by using the PM3 Hamiltonian in Hyperchem 5.0 (Hypercube Inc., Gainesville, FL). The initial temperatures are insensitive to the exact normal-mode frequencies, justifying the use of an empirical Hamiltonian. The results in Table 1 show that the initial vibrational temperature in the electronic ground state is approximately 1200 K for each nucleoside. Since vibrational cooling for both Ado and Cyd is substantially slower than internal conversion, photoproduct formation by hot ground-state molecules could be more important than reactions on the $S_1$ state surface. It was proposed earlier that pyrimidine photohydrates are formed from vibrationally hot molecules in $S_0$.[70] Additional work is required to fully determine whether thermal chemistry in $S_0$ can compete with the picosecond time scale of vibrational cooling.

Time constants obtained by fitting the decays for Ado in Figure 7 vary from 0.4 to 2.0 ps, depending on probe wavelength. This is considerably faster than cooling rates reported in other molecules. For example, cooling times of ≈10 ps were measured for azulene in a variety of nonaqueous solvents.[59−61] The much faster cooling rates for the nucleosides arise in our opinion from hydrogen bonding to water molecules, which provide efficient pathways for intermolecular vibrational energy flow to the solvent. Evidence that H-bonds can accelerate vibrational cooling comes from a study of azulene by Troe and co-workers.[60] They observed cooling in 3.3 ps in a 1:3 methanol/water mixture, faster than in any of the solvents in their study, and considerably faster than cooling in neat methanol ($\tau = 8.3$ ps). Terazima has shown recently that the number of solvent OH groups per unit volume correlates well with the vibrational cooling rates for betaine-30, following $S_3/S_0$ internal conversion.[71] A variety of other studies have found evidence for ultrafast vibrational energy relaxation through hydrogen bonds.[72−76] The ease of observing vibrational cooling in the nucleobases and their large number of hydrogen-bonding sites may make the DNA and RNA bases good model compounds for testing the dependence of vibrational cooling on hydrogen bonding.

In addition to hot ground-state absorption, there are two other contributions to the UV signals. Absorption by $e_{aq}^-$ produced by the two-photon ionization of water is again responsible for long-time signal offsets. Because absorption by $e_{aq}^-$ is much weaker in the UV, offsets are significant only for the high pump intensity used to record the transients in Figure 8. In this figure, it is also evident that the offset is larger for longer probe wavelengths, as expected from the absorption spectrum of $e_{aq}^-$. A second contribution is coherent (simultaneous) absorption of one pump photon and one probe photon near $t = 0$, as first described by Reuther et al.[38] This results in an instrument-limited spike, which is most obvious in the Cyd scans in Figure 8, but can also be seen at 270 nm in Figure 7. Since the cross-section for simultaneous absorption of two photons by water increases with the sum of the photon energies, the spike is larger at shorter probe wavelengths. Interestingly, the UV signals do not show clear evidence of a bleach recovery, even at 270 and 280 nm, where the bases show significant ground-state absorption. This may be due to interference by the coherent absorption spike, and our somewhat poorer time resolution (200−300 fs) at UV probe wavelengths.

**Comparison to Previous Lifetime Measurements.** The $S_1$ lifetimes reported here are significantly faster than all previously reported values from time-resolved measurements. Excited-state deactivation in the nucleosides occurs in hundreds of femtoseconds, and not in the 1−10 ps range, as most widely discussed in the past. The streak cameras used by others[45,77,78] lack sufficient temporal resolution to capture the subpicosecond excited-state decays reported here. Previous pump−probe studies[35,38,39,79,80] were similar in spirit to ours, but they did not identify ESA, and instead focused on dynamics in the UV. As we have shown, this spectral region is dominated by ground-state vibrational cooling dynamics. These more slowly decaying signals provide no information about the internal conversion dynamics. Furthermore, the past pump−probe studies used intensities that are 1−2 orders of magnitude higher than the ones used here. These high intensities produce substantial multiphoton excitation, which greatly complicates the analysis. Reuther et al. recently reported $\tau \approx 1$ ps for A, C, T, and U based on analysis of their data using a 7-level kinetic scheme.[39] In contrast, our lifetimes were obtained by globally fitting a single exponential directly to our experimental transients. Our results show that each base has a characteristic decay time. According to our lifetime ordering (A < G ≤ T < C), nonradiative decay is faster for the purines than for the pyrimidines. This is consistent with the purine bases' lower propensity for photodamage, and validates the notion that

(68) Elsaesser, T.; Kaiser, W. *Annu. Rev. Phys. Chem.* **1991**, *42*, 83.
(69) Owrutsky, J. C.; Raftery, D.; Hochstrasser, R. M. *Annu. Rev. Phys. Chem.* **1994**, *45*, 519.
(70) Fisher, G. J.; Johns, H. E. In *Photochemistry and Photobiology of Nucleic Acids*; Wang, S. Y., Ed.; Academic Press: New York, 1976; Vol. 1, p 169.
(71) Woutersen, S.; Bakker, H. J. *Nature (London)* **1999**, *402*, 507.
(72) Terazima, M. *Chem. Phys. Lett.* **1999**, *305*, 189.
(73) Laenen, R.; Gale, G. M.; Lascoux, N. *J. Phys. Chem. A* **1999**, *103*, 10708.
(74) Laenen, R.; Simeonidis, K. *Chem. Phys. Lett.* **1998**, *292*, 631.
(75) Terpstra, P. A.; Otto, C.; Greve, J. *Biopolymers* **1997**, *41*, 751.
(76) Bonn, M.; Brugmans, M. J. P.; Kleyn, A. W.; van Santen, R. A. *Chem. Phys. Lett.* **1995**, *233*, 309.
(77) Häupl, T.; Windolph, C.; Jochum, T.; Brede, O.; Hermann, R. *Chem. Phys. Lett.* **1997**, *280*, 520.
(78) Plessow, R.; Brockhinke, A.; Eimer, W.; Kohse-Hoinghaus, K. *J. Phys. Chem. B* **2000**, *104*, 3695.

photodamage is minimized when the rate of nonradiative decay is maximized.

Subpicosecond decays in the visible and the slower hot ground-state dynamics in the UV provide a consistent picture that argues for the accuracy of our measured lifetimes. Further support comes from good agreement with estimates based on the known fluorescence quantum yields. The fluorescence lifetime, $\tau_F$, of any fluorophore can be calculated from the fluorescence quantum yield, $\phi_F$, by the relation $\tau_F = \phi_F\tau_0$, where $\tau_0$ is the radiative lifetime. The radiative lifetime can be estimated by using the Strickler−Berg formula[81] and the stationary absorption spectrum. There is considerable uncertainty in this procedure due to the difficulty of isolating the lowest absorption band in a UV−vis spectrum. Nevertheless, estimates of the radiative lifetime, $\tau_0$, of the DNA bases between 3 and 8 ns were published by Callis.[82] Even with the longer value of 8 ns and the known values of $\phi_F$ for the nucleosides, subpicosecond lifetimes are predicted. On the basis of their estimates of the radiative lifetimes, Vigny and Duquesne reported $\tau_F$ values of 0.3, 0.5, 0.8, and 1.0 ps for the nucleotides AMP, GMP, TMP, and CMP in 1976.[32] The lifetime ordering is the same as ours, and the absolute values agree quiet well, particularly for the purines.

**Mechanistic Implications.** Our measurements show that excited state decay occurs in hundreds of femtoseconds for Ado, Guo, Cyd, and Thd. Since transients at UV wavelengths that lie within the ground state absorption spectrum recover completely within a few picoseconds, proposed mechanisms that involve relaxation to a long-lived dark state[83] can be ruled out. Instead, the evidence overwhelmingly supports ultrafast return to $S_0$. It is impossible to explain subpicosecond rates of internal conversion by using the energy gap law. The average energy gap between the $S_0$ and $S_1$ states of the different nucleobases at room temperature is $\approx$34 000 cm$^{-1}$ as determined from the emission spectra in water.[24] There is no correlation between the ordering of the $S_1$ state energies at 300 K, G < C ≤ T < A,[26] and the ordering of $S_1$ lifetimes reported here, A < G ≤ T < C. In fact, Ado, the nucleoside with the largest 0−0 transition energy in aqueous solution, has the highest rate of internal conversion.

Initial motion on the excited state surface must rapidly move the initial wave packet toward a geometry where the energy gap with $S_0$ is much smaller, if indeed a gap exists at all. We suggested previously[5] that a conical intersection could explain ultrafast excited-state decay, as has been found, for example, for azulene.[84] Lim has described how vibronic coupling between energetically nearby n−$\pi$* and $\pi$−$\pi$* states can reduce the energy gap to the ground state and provide a mechanism ("proximity effect") for efficient fluorescence quenching in nitrogen heterocyclic compounds.[85] This mechanism, although it does not require conical intersection between $S_0$ and $S_1$, has been mentioned in the past as an explanation of the short lifetimes of the DNA bases.[34,86] Ab initio calculations by Broo have provided some qualitative support for this mechanism.[87] Using CASSCF, CIS, and AM1 methods, Broo found strong mixing between the lowest n−$\pi$* and $\pi$−$\pi$* states of adenine. Ring puckering in the six-membered ring of adenine (particularly at N1−C2−N3) was identified as the coordinate that transforms the initially planar $\pi$−$\pi$* state into the nonplanar n−$\pi$* state. The quasistationary points corresponding to these two states are close in energy and separated by a small barrier of just 0.6 kJ mol$^{-1}$. Out-of-plane distortion leads to increased overlap with the $S_0$ vibrational states. The resulting large Franck−Condon factors lead to rapid radiationless decay.

A further possibility is that photochemical rearrangement occurs during excited-state decay. Decay from $S_1$ might then occur by conical intersection to the electronic surface of a transient intermediate, which subsequently relaxes to $S_0$. Domcke and co-workers proposed such a mechanism to explain nonradiative decay in pyridine and other azines.[88] They suggested that electrocyclic ring-closing in $S_1$ produces a prefulvene-like intermediate, which subsequently re-aromatizes in a barrierless process to regenerate the electronic ground state. This de-aromatization → re-aromatization process provides a photochemical alternative to the purely photophysical picture of Lim. Chachisvillis and Zewail recently invoked a similar concept to explain their ultrafast measurements of pyridine dynamics in solution.[89] It is possible that a similar mechanism could be operative in the DNA bases. High-quality ab initio calculations of the excited states will be required to decide this issue. In any event, the speed of excited state decay suggests that it occurs by a substantially barrierless process.

**Implications for Molecular Evolution.** Photodamage rates to DNA and RNA would be significantly higher in the absence of ultrafast nonradiative decay by the bases. Greater genomic photostability is advantageous, and this observation has interesting implications for the origin of life and the evolution of biomolecules. The DNA and RNA bases have essentially the same photophysical properties as sunscreens that function by absorption. Such sunscreens nonradiatively dissipate potentially damaging electronic energy rapidly and with high efficiency.[90] By converting potentially damaging electronic energy into vibrational energy (i.e. heat) in $S_0$ in hundreds of femtoseconds, the nucleobases provide passive photoprotection like other natural compounds such as the flavonoids of plants,[91] cyanobacterial pigments such as scytonemin,[92] and the mycosporine-like amino acids.[93]

The photoprotective properties of the DNA bases would have been especially important at the dawn of life on earth. Current evidence suggests that life arose a billion or more years before the presence of a significant stratospheric ozone layer. Today's ozone layer provides nearly total attenuation of UV light at $\lambda$ < 295 nm at earth's surface, restricting electronic excitation of the bases to their long-wavelength absorption tails, where the absorption cross sections are smaller. On the other hand, the high, and spectrally uniform fluence of short-wavelength UV light during the Archean era would have posed a grave threat to the earliest life forms.[94] Ultrafast nonradiative decay would have been an essential molecular survival mechanism, particularly at the earliest times before the appearance of the complex enzymes necessary for active repair of photodamaged nucleic acids. In their role as "primordial sunscreens" the

(79) Oraevsky, A. E.; Nikogosyan, D. N. *Chem. Phys.* **1985**, *100*, 429.
(80) Nikogosyan, D. N.; Görner, H. *J. Photochem. Photobiol. B: Biol.* **1992**, *13*, 219.
(81) Strickler, S. J.; Berg, R. A. *J. Chem. Phys.* **1962**, *37*, 814.
(82) Callis, P. R. *Chem. Phys. Lett.* **1979**, *61*, 563.
(83) Lee, Y. J.; Summers, W. A.; Burr, J. G. *J. Am. Chem. Soc.* **1977**, *99*, 7679.
(84) Bearpark, M. J.; Bernardi, F.; Clifford, S.; Olivucci, M.; Robb, M. A.; Smith, B. R.; Vreven, T. *J. Am. Chem. Soc.* **1996**, *118*, 169.
(85) Lim, E. C. *J. Phys. Chem.* **1986**, *90*, 6770.
(86) Lai, T.-I.; Lim, B. T.; Lim, E. C. *J. Am. Chem. Soc.* **1982**, *104*, 7631.
(87) Broo, A. *J. Phys. Chem. A* **1998**, *102*, 526.
(88) Sobolewski, A. L.; Domcke, W. *Chem. Phys. Lett.* **1991**, *180*, 381.
(89) Chachisvillis, M.; Zewail, A. H. *J. Phys. Chem. A* **1999**, *103*, 7408.
(90) Kimbrough, D. R. *J. Chem. Educ.* **1997**, *74*, 51.
(91) Caidwell, M. M.; Robberrecht, R.; Flint, S. D. *Physiol. Plant.* **1983**, *58*, 445.
(92) Garcia-Pichel, F.; Castenholz, R. W. *J. Phycol.* **1991**, *27*, 395.
(93) Bandaranayake, W. M. *Nat. Prod. Rep.* **1998**, *15*, 159.
(94) Cockell, C. S. *Orig. Life Evol. Biosph.* **2000**, *30*, 467.

nucleobases may have provided essential photoprotection as components of the first self-replicating biomolecules on the early earth. Sunscreen-like functionality may have been just as important for the adoption of the bases as the building blocks of the genetic code as their ability to noncovalently associate through hydrogen bonding. From this viewpoint, nonradiative decay may be as highly evolved in nature as the better-known ultrafast biological photoprocesses[95] of visual signal transduction, light harvesting, and electron transfer in the photosynthetic reaction center.

## Conclusions

Excited state decay by common nucleosides occurs in hundreds of femtoseconds by internal conversion to the electronic ground state. Two spectrally distinct regions of transient absorption have been identified. Excited-state absorption by the $S_1$ state of each nucleoside is characterized by a broad, but weak absorption band centered near 600 nm, which decays in hundreds of femtoseconds by internal conversion. Signals in the UV reveal the subsequent dynamics of vibrational cooling in the electronic ground state. Vibrational cooling for Ado occurs in $\leq 2$ ps, considerably slower than the initial relaxation to $S_0$. The vibrational cooling rate is, however, substantially faster than commonly observed for hydrocarbons in nonaqueous solvents, suggesting that solute−solvent H-bonds provide efficient pathways for intermolecular vibrational energy transfer. The ability to directly observe excited state dynamics in the DNA bases, as demonstrated here, should significantly advance understanding of the mechanism underlying their ultrafast nonadiabatic dynamics. We anticipate that the techniques described here for studying the photophysics of monomeric bases will be useful for studying the excited-state dynamics of oligo- and polynucleotides. Such studies will provide insight into how base stacking and base pairing influence energy relaxation, and may explain the sequence-dependent quantum yields of certain DNA photoproducts.

JA0161453

(95) Ratner, M. A. *Proc. Natl. Acad. Sci. U.S.A.* **2001**, *98*, 387.